

Specific Features of Magnetic Properties of Ferrihydrite Nanoparticles of Bacterial Origin: A Shift of the Hysteresis Loop

D. A. Balaev^{a, b, *}, A. A. Krasikov^b, A. A. Dubrovskiy^{a, c}, S. V. Semenov^{a, b}, S. I. Popkov^{a, b},
S. V. Stolyar^{a, b}, R. S. Iskhakov^a, V. P. Ladygina^d, and R. N. Yaroslavtsev^b

^a Kirensky Institute of Physics, Siberian Branch of the Russian Academy of Sciences,
Akademgorodok 50/38, Krasnoyarsk, 660036 Russia

^b Siberian Federal University, Svobodny pr. 79, Krasnoyarsk, 660041 Russia

^c International Laboratory of High Magnetic Fields and Low Temperatures, ul. Gajowicka 95, Wroclaw, 53-421 Poland

^d International Scientific Centre for Organism Extreme States Research,
Presidium of the Krasnoyarsk Scientific Centre of the Siberian Branch of the Russian Academy of Sciences,
Akademgorodok 50, Krasnoyarsk, 660036 Russia

* e-mail: dabalaev@iph.krasn.ru

Received July 9, 2015

Abstract—The results of the experimental investigation into the magnetic hysteresis of systems of superparamagnetic ferrihydrite nanoparticles of bacterial origin have been presented. The hysteresis properties of these objects are determined by the presence of an uncompensated magnetic moment in antiferromagnetic nanoparticles. It has been revealed that, under the conditions of cooling in an external magnetic field, there is a shift of the hysteresis loop with respect to the origin of the coordinates. These features are associated with the exchange coupling of the uncompensated magnetic moment and the antiferromagnetic “core” of the particles, as well as with processes similar to those responsible for the behavior of minor hysteresis loops due to strong local anisotropy fields of the ferrihydrite nanoparticles.

DOI: 10.1134/S1063783416020050

1. INTRODUCTION

In recent years, considerable interest expressed in the study of antiferromagnetic (AF) nanoparticles is associated with their unusual magnetic properties, which are cardinally different from the magnetic properties of the corresponding bulk antiferromagnetic materials [1]. The main difference is that nanoparticles acquire an uncompensated magnetic moment μ_{unc} due to the presence of defects and the appearance of surface effects caused, for example, by an odd number of antiferromagnetic sublattices. It turned out that the uncompensated magnetic moment μ_{unc} for particles with the size of a few nanometers can reach a few hundred Bohr magnetons, which already is comparable to the magnetic moment of ferromagnetic (FM) particles of the same size [1, 2]. For practical applications of magnetically active nanoparticles, such as, for example, the targeted drug delivery in the human body, antiferromagnetic nanoparticles can successfully “compete” with ferrimagnetic “analogs.” The appearance of an uncompensated magnetic moment in the system of antiferromagnetic nanoparticles leads to a superparamagnetic behavior of the system with a characteristic blocking temperature T_B and hysteresis loops of the magnetization at temperatures $T < T_B$. More-

over, in these systems, there is a shift of the magnetic hysteresis loop under the conditions of cooling in an external magnetic field.

A shift of magnetic hysteresis loops is characteristic of objects containing interfaces between the ferromagnetic and antiferromagnetic phases and results from their exchange coupling. Although the exchange shift of hysteresis loops was found in the 1950s of the last century [3] and had been studied both on thin-film layered structures and on bulk heterophase materials [4], in recent years, because of possible practical applications, this phenomenon has been actively investigated on magnetic nanoparticles [5]. It is worth noting that, even though magnetic nanoparticles are chemically homogeneous, their surface atoms can exhibit magnetic properties different from those of the “core” of a nanoparticle with the possible implementation of the mechanism of exchange coupling between the “core” and the surface of the nanoparticle [6–8].

To date, not all the specific features observed in the behavior of the magnetic properties of antiferromagnetic nanoparticles have been clearly understood [1, 9]. In this paper, we have presented the results of the investigation of the hysteretic behavior of a magnetic moment of ferrihydrite nanoparticles that are charac-

terized by an antiferromagnetic order [10, 11] and also demonstrate the effect of the shift of the magnetic hysteresis loop [9, 10, 12, 13]. The iron hydroxide under investigation has the nominal chemical formula $5\text{Fe}_2\text{O}_3 \cdot 9\text{H}_2\text{O}$ with the variable “water” content. Ferrihydrite either can be chemically synthesized or can be extracted from the waste products of the organisms. The best known commercial product is horse spleen ferritin in the form of a ferrihydrite particle within the protein shell with the inner diameter of 5–8 nm. In a series of studies [14–18], it was shown that ferrihydrite nanoparticles with the size of a few nanometers and the total number of iron atoms $N_{\text{Fe}} \sim 2000\text{--}2500$ can also be extracted from the waste products of the bacteria cultured under specific conditions. In our recent studies [19, 20], it was shown that the average size (or the number of iron atoms N_{Fe}) and the corresponding blocking temperatures of an ensemble of ferrihydrite nanoparticles of bacterial origin can be increased by a low-temperature heat treatment. In the present study, this allowed us to compare the parameters characterizing the shifts of magnetic hysteresis loops for ferrihydrite nanoparticles that have different average sizes.

2. EXPERIMENT

2.1. Samples

The *Klebsiella oxytoca* strain used for the preparation of ferrihydrite nanoparticles was isolated from sapropel of Lake Borovoe (Krasnoyarsk region, Russia). The microorganisms were grown under anaerobic conditions. Then, bacterial suspensions were subjected to repeated ultrasonic treatment followed by their washing and centrifuging with the formation of a stable sol of nanoparticles in an aqueous solution, which was subsequently dried. The described method [14, 15, 18] has made it possible to reproducibly obtain ferrihydrite nanoparticles, which was reliably identified from the analysis of the Mössbauer spectra.

The investigations were carried out on the initial powders of magnetic ferrihydrite nanoparticles from different batches of preparation, as well as on the samples subjected to low-temperature treatment in an air atmosphere at a temperature of 150°C for different times (up to 240 h). As was shown in our recent study [20], the performed annealing did not lead to the formation of other phases of iron oxide, but the blocking temperature of the nanoparticles increased due to their coarsening. In the present study, the ferrihydrite (FHYD) samples were designated as FHYD- X , where X is the temperature at which the temperature dependence of the magnetic moment $M(T)$ in the external magnetic field $H = 1$ kOe (under conditions of cooling in a zero external field) exhibits a maximum.

2.2. Magnetic Measurements

The magnetic measurements were performed on a vibrating-sample magnetometer [21]. The powder under investigation was fixed in a measuring cell filled with paraffin. The data corrected for the diamagnetic signal from the measuring cell with paraffin are presented below in units of emu per unit mass of the studied powder. The measurements were carried out in the modes of cooling without a magnetic field (zero field cooling (ZFC)) and cooling in a magnetic field (field cooling (FC)). The shift of the magnetic hysteresis loop was investigated after cooling under the FC conditions in the magnetic field $H = 30$ kOe down to the temperature of 4.2 K. Then, the dependence $M(H)$ was measured during cycling of the external magnetic field within the range of ± 30 kOe. The cooling in the magnetic field was performed from the temperature of 120 K, which is obviously higher than the temperature corresponding to the maximum in the dependence $M(T)$ and the temperature corresponding to the irreversible behavior of the dependences $M(T)$ measured under the ZFC and FC conditions. Under the ZFC conditions, the hysteresis loops were measured to different maximum values of the applied magnetic field H_{max} .

3. RESULTS AND DISCUSSION

The hysteretic dependences $M(H)$ of the FHYD26 sample measured under the conditions of ZFC ($H_{\text{max}} = 30$ kOe) and FC are shown in Fig. 1a. As is clearly seen from this figure, there is a shift of the magnetic hysteresis loop measured under the FC conditions along both the horizontal axis (H) and the vertical axis (M). Figure 1b illustrates the above behavior of the dependence $M(H)$ on an enlarged scale together with a fragment of the hysteresis loop at the value of $H_{\text{max}} = 60$ kOe. For the FC conditions, we introduce the following notation: the “coercive forces” $H_{\text{CL}}(\text{FC})$ and $H_{\text{CR}}(\text{FC})$ correspond to the magnetic fields in which the descending and ascending branches of the hysteresis loop, respectively, intersect the abscissa axis H . These designations and the coercive forces H_C for the magnetic fields $H_{\text{max}} = 30$ and 60 kOe are indicated in Fig. 1b. It can be seen that the value of $H_{\text{CL}}(\text{FC})$ exceeds the coercive force H_C for both the field $H_{\text{max}} = 30$ kOe and the field $H_{\text{max}} = 60$ kOe. At the same time, the shift of the ascending part of the hysteresis loop under the FC conditions is significantly smaller (the value of $H_{\text{CR}}(\text{FC})$ is close enough to the value of $H_C(H_{\text{max}} = 30$ kOe)).

The described behavior is also characteristic of the samples with a higher blocking temperature. The obtained data for the FHYD78 sample ($T_B \approx 78$ K) are presented in Fig. 2. This figure shows the dependence $M(H)$ plotted on an enlarged scale for the FC mode in the magnetic field $H = 30$ kOe together with the hys-

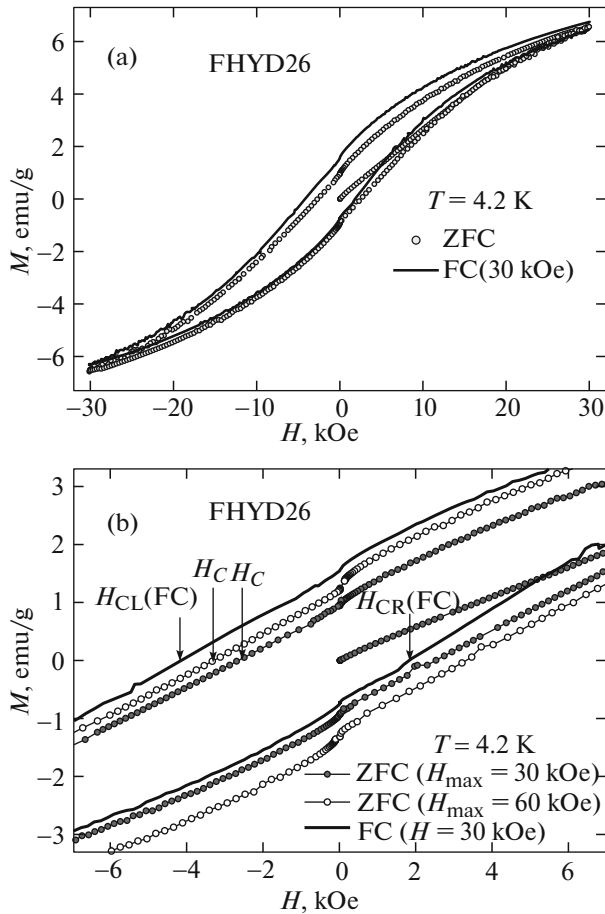


Fig. 1. (a) Hysteresis loops of the FHYD26 sample in the modes FC ($H_{FC} = 30$ kOe) and ZFC (in the maximum applied magnetic fields $H_{max} = 30$ and 60 kOe) at the temperature $T = 4.2$ K. (b) The same dependences plotted on an enlarged scale in the vicinity of the origin of the coordinates with examples of determining the values of H_C , $H_{CL}(FC)$, and $H_{CR}(FC)$.

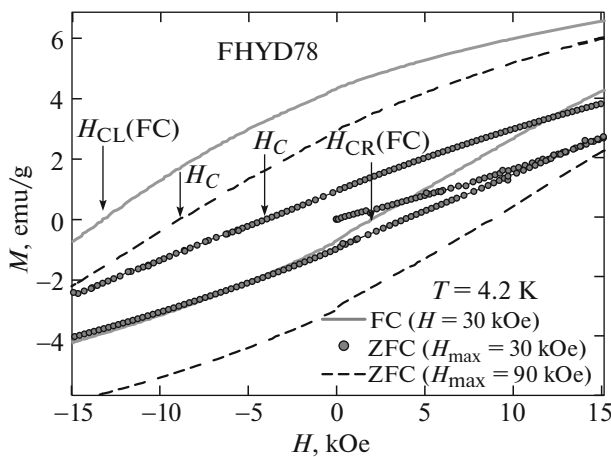


Fig. 2. Details of the hysteresis loops at the temperature $T = 4.2$ K for the FHYD78 sample in the modes FC ($H_{FC} = 30$ kOe) and ZFC (in the maximum applied magnetic fields $H_{max} = 30$ and 90 kOe) in the vicinity of the origin of the coordinates.

teresis loops measured for the values of $H_{max} = 30$ and 90 kOe.

In order to quantitatively describe the shift of the magnetic hysteresis loop, we used the quantity characterizing the shift of the dependence $M(H)$ along the abscissa axis with respect to the origin of the coordinates [4, 5]. In the notation introduced above, this quantity is expressed as follows: $H_{SH} = \{|H_{CL}(FC)| + |H_{CR}(FC)|\}/2$. From the analysis of the data presented in Figs. 1 and 2, we find the values of $H_{SH} \approx 3.0$ and 7.6 kOe for the FHYD26 and FHYD78 samples, respectively; i.e., the shift of the hysteresis loop increases with an increase in the blocking temperature T_B or with an increase in the particle size. This tendency holds for all the samples under investigation. The dependence $H_{SH}(T_B)$ is illustrated in Fig. 3.

There are at least two reasons for this behavior. The first reason is associated with the mechanism of exchange coupling between the antiferromagnetic and ferromagnetic phases in the nanoparticles. The other possible reason is that the dependences $M(H)$ measured in the FC mode reflect the behavior of the minor hysteresis loops. Let us consider these mechanisms in more detail.

3.1. Exchange Bias

The classical mechanism of exchange coupling in a ferromagnetic/antiferromagnetic structure implies that an additional source of unidirectional magnetic anisotropy, which results in the shift of the magnetic hysteresis loop, arises during cooling of the ferromagnetic/antiferromagnetic structure in an external magnetic field from the temperature above the Néel temperature of the antiferromagnet [4, 5]. The interaction

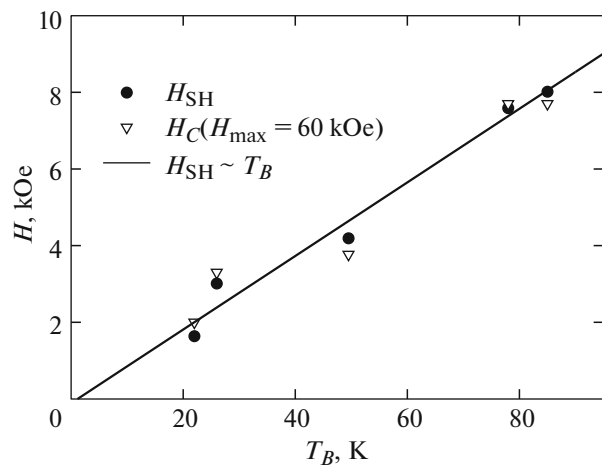


Fig. 3. Dependences of the hysteresis loop shift H_{SH} in the FC mode ($H_{FC} = 30$ kOe) and the coercive force H_C in the ZFC mode (at $H_{max} = 60$ kOe and $T = 4.2$ K) on the blocking temperature for the studied samples. The straight line shows the approximation of the data on $H_{SH}(T_B)$ by a linear dependence.

between the magnetic moments of the surface and the “core” of a particle is considered as applied to magnetic nanoparticles. If the “core” of the nanoparticle is ferromagnetic or ferrimagnetic, the surface spins can exhibit a spin-glass behavior [4–6]. For antiferromagnetic particles, the uncompensated magnetic moment, in many cases, is formed by surface atoms, which are also characterized by a spin-glass behavior. For these systems, the exchange interaction leads to a shift of the magnetic hysteresis loop with cooling in an external magnetic field from the temperature above the blocking temperature.

The exchange bias field H_{EB} for ferromagnetic/antiferromagnetic structures is determined by the following relationship between the parameters of the antiferromagnet (the exchange constant A_{AF} and the anisotropy constant K_{AF}) and the ferromagnet (the saturation magnetization M_{FM} and the thickness of the ferromagnetic layer d_{FM} [4, 5]):

$$H_{EB} = 2(A_{AF}K_{AF})^{1/2}/M_{FM}d_{FM}. \quad (1)$$

For the studied samples, the blocking temperature is accurately determined. Therefore, in this case, we obtain the dependence of the exchange bias field H_{EB} on this temperature.

Ferrihydrite is antiferromagnetically ordered and has an uncompensated magnetic moment. As a result, the magnetization curve is determined by the superposition of two contributions: the ferromagnetic contribution (hysteresis at $T < T_B$) with signs of the tendency to saturation in strong magnetic fields and the linear-in-field contribution due to the magnetic susceptibility of the antiferromagnet [1, 7, 12, 18, 19] (see also Fig. 1a). It is clear that the ferromagnetic contribution is associated with the uncompensated magnetic moment μ_{unc} . Moreover, the investigations of the magnetic properties of ferritin and ferrihydrite nanoparticles [1, 10, 12, 18, 19, 22] demonstrated that

$$\mu_{unc} \sim N_{Fe}^{1/2}, \quad (2)$$

where N_{Fe} is the number of iron atoms in a particle. Since the saturation magnetization is determined by the formula $M_{FM} = \mu_{unc}/V$, where V is the particle volume and $V \sim N_{Fe}$, we obtain $M_{FM} \sim N_{Fe}^{-1/2} \sim V^{-1/2}$.

As regards the possible variation in the ferromagnetic layer thickness d_{FM} involved in expression (1) for the samples under investigation, it can be assumed that $d_{FM} \approx \text{const}$. Indeed, according to the classical treatment proposed by Néel, if the antiferromagnetic particle satisfies relationship (2), the ferromagnetic contribution is caused by defects of the antiferromagnetic ordering on the surface and in the bulk of the particle. For the studied samples with the blocking temperature $T_B \sim 20$ K, the number of iron atoms N_{Fe} is equal to $\sim 2.5\text{--}3.0 \times 10^3$ [17, 18]. Therefore, the number of ferromagnetically ordered atoms is ~ 50 ,

which corresponds to $\sim 2\%$ of the number of iron atoms N_{Fe} and to $\sim 4\%$ of the number of surface atoms (for the cubic form). With an increase in the number of iron atoms N_{Fe} , the fraction of ferromagnetically ordered atoms will decrease. Hence, it is unlikely that the thickness of the ferromagnetic layer will radically change.

The volume of the particles is related to the blocking temperature T_B according to the Néel–Brown formula [1] as follows:

$$T_B \approx K_{AF}V/25k. \quad (3)$$

In this expression, k is the Boltzmann constant and the factor of ≈ 25 in the denominator corresponds to the logarithm of the ratio of the characteristic times of static magnetic measurements and superparamagnetic particle relaxation. When condition (2) and, consequently, the relationship $M_{FM} \sim V^{-1/2}$ are satisfied, from expressions (1) and (3) we can easily find that

$$H_{EB} \sim T_B^{1/2}.$$

The dependence $H_{SH}(T_B)$ plotted from the data presented in Fig. 3 is best described by the linear relationship $H_{SH} \sim T_B^a$ (where $a \approx 0.8\text{--}1.0$); i.e., despite some scatter of the experimental points for the samples of different batches of preparation, it can be argued that, with an increase in the blocking temperature T_B , the shift of the magnetic hysteresis loop increases more rapidly than expected for the exchange shift mechanism. The latter circumstance can indicate an additional contribution to the observed effect, which, most likely, can be caused by the so-called “minor loop effect” [23].

3.2. Minor Loop Effect

If the strength of the magnetic field, in which the measurements are carried out in the FC mode, is less than that of the magnetic field corresponding to the irreversible behavior of the dependence $M(H)$, then the FC conditions can be considered as an analog of the ZFC conditions, and the observed shift of the hysteresis loop in this case can reflect the behavior of minor hysteresis loops. In fact, the magnetic hysteresis loops of ferrihydrite nanoparticles at low temperatures are usually characterized by very high values of the irreversibility fields [9, 19]; moreover, in magnetic fields H_{max} of the order of 60–90 kOe, the hysteresis loops remain open [9, 19], which is also the case for the samples investigated in this work. Consequently, the coercive force H_C depends on the value of H_{max} , which is seen from the data presented in Figs. 1 and 2. Figure 4 illustrates the dependence of the coercive force H_C on the maximum applied magnetic field H_{max} for the FHYD78 sample at $T = 4.2$ K.

In turn, the coercive force H_C at a fixed value of H_{max} depends on the blocking temperature of the sam-

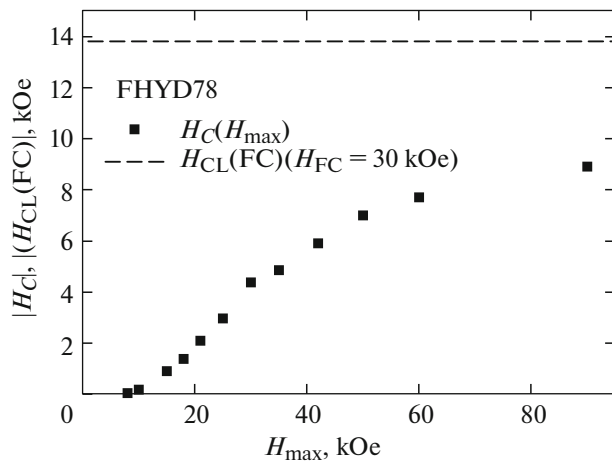


Fig. 4. Dependences of the coercive force H_C under the ZFC conditions at $T = 4.2$ K on the maximum applied magnetic field H_{\max} for the FHYD78 sample. The horizontal dashed straight line corresponds to the field $H_{CL}(FC)$ (at $H_{FC} = 30$ kOe) for this sample.

ples, i.e., on the particle size. In addition to the dependence $H_{SH}(T_B)$, Fig. 3 shows the values of H_C ($H_{\max} = 60$ kOe) for the samples under investigation. It can be seen from this figure that the dependences $H_{SH}(T_B)$ and $H_C(T_B)$ correlate with each other. Therefore, an increase in the blocking temperature T_B also leads to an increase in the coercive force of the limiting hysteresis loop H_C^* . Then, for the samples with a higher blocking temperature, the measurements in the FC mode are performed at a lower value of H_{FC}/H_C^* , and the influence of the “minor hysteresis effect” will be more pronounced. Thus, the observed shift of the hysteresis loop and rather strong dependence $H_{SH} \sim T_B$ can be associated with the behavior similar to that of the minor hysteresis loops.

It should be noted that we cannot draw a complete analogy of the behavior of the minor hysteresis loops of the ferromagnet, which are determined by the motion of the domain walls, with the system under investigation. For an ensemble of antiferromagnetic nanoparticles, the hysteretic behavior is caused by the hopping of the vector of the particle magnetic moment (μ_{unc}) through the energy barriers due to the magnetic anisotropy [9], even though the FC conditions can be considered as an analog of the application of a significantly stronger magnetic field under the ZFC conditions.

Let us now consider the relationship between the observed coercive force $H_{CL}(FC)$ and the dependence $H_C(H_{\max})$ shown in Fig. 4. The experimental dependence $H_C(H_{\max})$ has the form of an S-shaped curve with signs of the tendency to saturation in strong magnetic fields. It can be seen that the values of $H_{CL}(FC)$ in the field $H_{FC} = 30$ kOe are much higher than the

data on the dependence $H_C(H_{\max})$ in the high-field range, although this dependence is very difficult to extrapolate to the range of magnetic fields of several hundred kilooersteds for the purpose of evaluating the quantity H_C^* . Therefore, the observed shift of the hysteresis loop under the FC conditions should not be related only to the effects associated with the minor hysteresis loops. Apparently, the two mechanisms considered above contribute to the experimentally observed shift of the hysteresis loop.

4. CONCLUSIONS

Ferrihydrite nanoparticles that exhibit a superparamagnetic behavior demonstrate the effect of the shift in the magnetic hysteresis loop with cooling in an external magnetic field from a temperature that exceeds the blocking temperature. The quantity that characterizes the shift of the hysteresis loop with respect to the origin of the coordinates (H_{SH}) increases with an increase in the blocking temperature of the particles. In this case, the dependence $H_{SH}(T_B)$ for the same values of $H_{FC} = 30$ kOe is an approximately linear function.

The analysis of the obtained data revealed that the observed shift of the hysteresis loop can be associated with the following two mechanisms: (1) processes similar to those responsible for the behavior of minor hysteresis loops and (2) exchange coupling between the ferromagnetic phase (the uncompensated magnetic moment responsible for the superparamagnetic behavior) and the antiferromagnetic “core” of the particles. Presumably, these two mechanisms coexist with each other, and the determination of their contributions requires further investigation.

ACKNOWLEDGMENTS

This study was supported by the Ministry of Education and Science of the Russian Federation within the state contract for 2014–2016.

REFERENCES

1. S. Mørup, D. E. Madsen, C. Fradsen, C. R. H. Bahl, and M. F. Hansen, *J. Phys.: Condens. Matter* **19**, 213202 (2007).
2. Yu. L. Raikher and V. I. Stepanov, *J. Exp. Theor. Phys.* **107** (3), 435 (2008).
3. W. P. Meiklejohn and C. P. Bean, *Phys. Rev.* **102**, 1413 (1956).
4. J. Nogués and I. K. Schuller, *J. Magn. Magn. Mater.* **192**, 203 (1999).
5. J. Nogués, J. Sort, V. Langlais, V. Skumryev, S. Suriñach, J. S. Muñoz, and M. D. Baró, *Phys. Rep.* **422**, 65 (2005).
6. R. H. Kodama and A. E. Berkowitz, *Phys. Rev. B: Condens. Matter* **59**, 6321 (1999).

7. S. A. Makhlof, H. Al-Attar, and R. H. Kodama, *Solid State Commun.* **145**, 1 (2008).
8. A. Punnoose and M. S. Seehra, *Appl. Phys.* **91** (10), 7766 (2002).
9. N. J. O. Silva, V. S. Amaral, A. Urtizberera, R. Bustamante, A. Millan, F. Palacio, E. Kampert, U. Zeitler, S. de Brion, O. Iglesias, and A. Labarta, *Phys. Rev. B: Condens. Matter* **84**, 104427 (2011).
10. S. A. Makhlof, F. T. Parker, F. E. Spada, and A. E. Berkowitz, *J. Appl. Phys.* **81** (8), 5561 (1997).
11. M. S. Seehra, V. S. Babu, A. Manivannan, and J. W. Lynn, *Phys. Rev. B: Condens. Matter* **61**, 3513 (2000).
12. A. Punnoose, T. Phanthavady, M. S. Seehra, N. Shah, and G. P. Huffman, *Phys. Rev. B: Condens. Matter* **69**, 054425 (2004).
13. T. S. Berquó, J. J. Erbs, A. Lindquist, R. L. Penn, and S. K. Banerjee, *J. Phys.: Condens. Matter* **21**, 176005 (2009).
14. S. V. Stolyar, O. A. Bayukov, Yu. L. Gurevich, E. A. Denisova, R. S. Iskhakov, V. P. Ladygina, A. P. Puzyr', P. P. Pustoshilov, and M. A. Bitekhtina, *Inorg. Mater.* **42** (7), 763 (2006).
15. S. V. Stolyar, O. A. Bayukov, Yu. L. Gurevich, V. P. Ladygina, R. S. Iskhakov, and P. P. Pustoshilov, *Inorg. Mater.* **41** (6), 638 (2007).
16. Yu. L. Raikher, V. I. Stepanov, S. V. Stolyar, V. P. Ladygina, D. A. Balaev, L. A. Ishchenko, and M. Balasoiu, *Phys. Solid State* **52** (2), 298 (2010).
17. M. Balasoiu, S. V. Stolyar, R. S. Iskhakov, L. A. Ischenko, Y. L. Raikher, A. I. Kuklin, O. L. Orelovich, Yu. S. Kovalev, and T. S. Kurkin, *Rom. J. Phys.* **55** (7–8), 782 (2010).
18. D. A. Balaev, A. A. Dubrovskii, A. A. Krasikov, S. V. Stolyar, R. S. Iskhakov, V. P. Ladygina, and E. D. Khilazheva, *JETP Lett.* **98** (3), 139 (2013).
19. D. A. Balaev, A. A. Krasikov, A. A. Dubrovskii, S. V. Semenov, O. A. Bayukov, S. V. Stolyar, R. S. Iskhakov, V. P. Ladygina, and L. A. Ishchenko, *J. Exp. Theor. Phys.* **119** (3), 479 (2014).
20. D. A. Balaev, A. A. Krasikov, A. A. Dubrovskii, O. A. Bayukov, S. V. Stolyar, R. S. Iskhakov, V. P. Ladygina, and R. N. Yaroslavtsev, *Tech. Phys. Lett.* **41** (7), 705 (2015).
21. A. D. Balaev, Yu. V. Boyarshinov, M. M. Karpenko, and B. P. Khrustalev, *Prib. Tekh. Eksp.*, No. 3, 167 (1985).
22. J. G. E. Harris, J. E. Grimaldi, D. D. Awschalom, A. Chileró, and D. Loss, *Phys. Rev. B: Condens. Matter* **60**, 3513 (1999).
23. S. Giri, M. Patra, and S. Majumdar, *J. Phys.: Condens. Matter* **23**, 073201 (2011).

Translated by O. Borovik-Romanova